UNCLASSIFIED

AD 405 695

DEFENSE DOCUMENTATION CENTER

FOR

SCIENTIFIC AND TECHNICAL INFORMATION

CAMERON STATION, ALEXANDRIA, VIRGINIA

UNCLASSIFIED

UNEDITED ROUGH DRAFT TRANSLATION

STUDY OF THERMAL ELECTRON EMISSION FROM A HOLLOW CATHODE

By: M. B. Pyt'yeva and Ye. M. Dubinina

English Pages: 12

Source: Russian periodical, Izvestiya akademii nauk SSSR, Seriya fizicheskaya, Vol. 26, No. 11, 1962, pp. 1343-1348.

T-74
SOV/48-62-26-11-

THIS TRANSLATION IS A RENDITION OF THE ORIGINAL FOREIGN TEXT WITHOUT ANY ANALYTICAL OR EDITORIAL COMMENT. STATEMENTS OR THEORIES ADVOCATED OR IMPLIED ARE THOSE OF THE SOURCE AND DO NOT NECESSARILY REFLECT THE POSITION OR OPINION OF THE FOREIGN TECHNOLOGY DIVISION.

PREPARED BY:

TRANSLATION SERVICES BRANCH
FOREIGN TECHNOLOGY DIVISION
WP-AFB, OHIO.

STUDY OF THERMAL ELECTRON EMISSION FROM A HOLLOW CATHODE

M. B. Pyt'yeva and Ye. M. Dubinina

Introduction

The great interest in hollow oxide cathodes which has again been noted recently [1, 2] has been brought on by the considerable current densities of cathode emission, by the low voltages at which they may be obtained, as well as by the small effective dimensions of the electron source and the insensitivity of the cathode to ionic bombardment [3]. However, the mechanism of its emission has not yet been sufficiently studied; visual investigation of the structure of the beam formed by a system with a hollow cathode attests to its complexity. An attempt has been made to explain current anomalies of the cathode on the basis of the structural characteristics of the beam. Thus we assumed the presence of two components, in the current from a hollow cathode, which may be separated by a strong longitudinal magnetic field [4].

I. Investigation of the Structure of the Beam

1. Design of the Test System

Figure 1 shows the gun with the hollow cathode whose beam was studied in the given work. Cathode K is a closed cylindrical cavity coated on the inside with oxide paste. Anode A and accelerating electrode B are diaphrams made of hollow tungsten mesh. The introduction of the accelerating electrode B is required by the method of investigation used. The distance between the anode and cathode is 3 mm.

2. Test Method

The distribution of current density in the beam was determined from an oscillogram of the probe current (Fig. 2). A long thin metal probe P was placed in the path of the electron beam and periodically intersected the electron beam normal to the direction of its motion [5]. The magnitude of the current reaching the probe at any given moment may be calculated from the equation

$$j(r_0) = 2(1-\sigma)\int_{r_0-\delta}^{R_i} j(r) r \arccos\frac{r_0-\delta}{r}dr - 2(1-\sigma)\int_{r_0+\delta}^{R_i} j(r) r \arccos\frac{r_0+\delta}{r}dr. \qquad (1)$$

Here σ is the coefficient of secondary probe emission, δ is the thickness of the probe, and r_0 is the coordinate of the position of the probe. Determination of the current density $j(r)$ thus involves solution of integral equation (1), this solution may be obtained with sufficient accuracy by the approximation method used in this work.

3. Distribution of Current Density in a Cross Section of the Beam over the Range of Anode Voltages from 50 to 1000 Volts.

Figure 3 shows the form of a typical oscillogram of the current and its associated current-density distribution in the cross section of the electron beam.

It was noted that there was a significant variation in current density distribution in the beam with a variation in drawing potential. The results of the treatment of the oscillograms may be summarized as follows. For low anode voltages (from 50 to 100 volts) the picture of the distribution of current in the cross-section of the beam (Fig. 4a) corresponds to an almost hollow beam. An increase in the potential within this range simply causes an increase in current density in the hollow beam and a slight expansion of the ring in the cross section, mainly on account of a reduction of the radius of the inner boundary of the ring. The development of the field, which corresponds to the variation of the anode voltage above 100 volts (Fig. 4b) also produces an increase in current density in the more central portions of the electron beam, while the change in current density in the ring section of the beam, beginning with 150 volts, slows down. As the potential increases, the boundary region, with current density which is constant with respect to voltage, advances along the radius toward the center. At 260 volts there is a relative maximum current density at the center of the cross section of the beam (Fig. 4c) which at 500 volts anode potential already significantly exceeds the magnitude of the maximum current density at the edge of the beam (Fig. 4d).

It should be noted that when the voltage was increased and the diameter of the beam varied, no other geometric characteristics of structure were observed. This indicates an insignificant angular

scattering of electrons flying from the cathode opening.

4. Structure of the Cross Section of the Electron Beam as a Function of the Degree of Heating of the Cathode

It is inconvenient to characterize the degree of heating of a hollow cathode by its temperature, since the latter is not uniform for different sections of the surface of the cathode. Therefore, for convenience, we will use as such a characteristic the filament power of the heater or the filament voltage. Figure 5 shows the nature of the distribution of current density in the cross section of the electron beam for cases of varying degrees of cathode heating. At low temperatures corresponding to a filament power of 6.4 watts the electron beam appears as a narrow compact cylindrical ray. Heating the cathode causes an increase in the diameter of the electron beam while the current density in the central regions of the cross section does not change. The boundary of the region which has a current density that does not change with temperature moves, with increasing temperature, from the center along the radius, and the diameter continues to increase. With a filament power of 13.6 watts a relative maximum current density appears at the edge of the beam and increases as it moves along the radius away from the center (Figs. 5c,5d). An increase in filament power above 20.4 watts does not alter the distribution of current density in the beam.

5. Structure of the Beam When Altering the Vacuum

All of the experiments described above were conducted at a pressure of $5 \cdot 10^{-8}$ to $1 \cdot 10^{-7}$ mm. To investigate operation of the cathode under varying vacuums conditions we analyzed probe-current oscillograms with increasing residual-gas pressure.

Up to a pressure of $1 \cdot 10^{-4}$ mm neither the form of the oscillogram nor the absolute magnitude of the current underwent any changes. A subsequent increase in pressure causes a variation of the outer, most distant from the axis, regions of the electron beam. The current density in these regions decreased, the beam contracted without significant changes in the near-axis regions. The character of the variation of current density in the cross section of the beam in this case resembles the corresponding variation in current density with a reduction of cathode temperature. This similarity may apparently be explained by the increased heat transfer caused by the decrease in vacuum. Therefore, in order to separate the cathode contamination effect from the thermal effect, it is necessary to control the temperature of the cathode, keeping it constant. In the present work such a possibility was not provided for.

II. Certain Observations Relative to the Mechanism of Emission from a Hollow Cathode

We will use the "3/2 law" for a flat diode in pure form in the case of zero initial electron velocities. Calculation of the Maxwellian distribution of thermal electrons with respect to velocities led, for a flat diode, to the formula

$$I = A\frac{(V + |V_{min}|)^{3/2}}{(d - d_{min})^2}, \qquad (2)$$

where V_{min} and d_{min} are the magnitude of minimum potential and the corresponding position of the virtual cathode, respectively.

Thus we will use the "3/2 law" for the case when the surface of the virtual cathode coincides with the emitting surface. This occurs for the majority of known cathode geometries, and therefore this law is practically satisfied. The hollow cathode has a very large space

charge. Therefore, before the surface of the virtual cathode draws near the emitting surface, V_{min} and d_{min} pass through a large range of values. The "3/2 law" can hardly be expected to be satisfied in view of this fact alone. In addition, the various parts of the surface of the cathode are located at such varied positions with respect to the anode that the quantities V_{min} and d_{min} will vary differently in different directions. This leads to the fact that the surface of the virtual cathode and the distribution of the potential on it will vary significantly with voltage and the distribution of beam electrons with respect to velocity depends on this fact.

Therefore there is no basis for expecting that the current of a hollow cathode will vary from the magnitude of the applied voltage according to the "3/2 law."

The real volt-ampere characteristic of a hollow cathode may be explained in the following way.

In the presence of weak drawing fields, as long as the virtual cathode is located in the aperture, the volt—ampere characteristic is described by the Langmuir law. According to the degree of drawing-off of the space charge, the current from the portions of the aperture closest to the anode are saturated. The edge of the region of saturation migrates with the voltage along the surface of the cathode, embracing the surface of the edge of the aperture (on which, during operation of the cathode, a microcrystalline oxide deposit is formed) and the regions of the upper base of the cavity near the aperture. Here the virtual cathode migrates into the cavity; its form changes, seeking to coincide with the form of the cathode cavity. This establishes a more intense moving away of the central portions of the virtual cathode from the anode (the case of a cylindrical cavity —

the height greater than the diameter). Therefore, the external portions of the electron flux consisting of electrons emitted from the upper base of the cathode cavity make the basic contribution to the current, which explains the formation of an almost hollow beam at low voltages. Passing into the cavity, the electrical field also draws off electrons emitted from the lateral walls. If the current from the edges of the aperture and the regions adjacent to it form an outer dense ring in the cross section of the beam, then the parts of the upper base more distant from the aperture are responsible for the inner parts of the electron flux. Finally, the maximum density at the center is produced by emission from the lateral walls (Fig. 6)

Thermal regularities reflect the fact that the various parts of the cathode surface are at different temperatures; in particular, the regions which are immediately adjacent to the aperture have the lowest temperature.

III. Volt-Ampere Characteristics of a Hollow Cathode at Audio Frequencies

The purpose of this study was to clarify the inertia properties of the hollow cathode and also to examine the volt-ampere characteristics for hysteresis. Figure 7 shows the circuit for recording dynamic characteristics of the system.

Varying the frequency of the anode voltage from 20 to 2000 cps has no influence on the volt-ampere characteristics of the diode. According to the form of the volt-ampere characteristic, owing to the rather abrupt variation of it slope, the rise of an unstable condition in the system which hysteresis usually accompanies may be doubted. However, the volt-ampere characteristics of the diode with a hollow

cathode, recorded with direct and reverse variation of voltage, practically coincide, which testified to the absence of hysteresis properties in the test circuit.

IV. Volt-Ampere Characteristics of the Hollow Cathode for Various Temperatures and Distances Between the Cathode and Anode

For greater accuracy, a circuit analogous to the one in Fig. 7 was used in this case to record characteristics.

Figure 8 shows the family of volt-ampere characteristics obtained for different heating of the cathode. It can be seen from the figure that for weak drawing fields the current from the hollow cathode is determined by the space charge. Moreover, for volt-ampere characteristics corresponding to a higher cathode temperature, the voltage range at which the current is determined by the space charge naturally increases.

Figure 9 shows the family of volt-ampere characteristics with the distance between the cathode and anode serving as the parameter and varying from 0.5 to 13 mm.

The current-stopping properties of a longitudinal magnetic field were also studied. It was established that current emitted from various sections of the surface of the cathode are cut off differently. Consequently, it is not possible in this way to separate completely the current emitted, let us say, by the edge of the aperture, from the current from within the cavity.

Conclusions

1. Electrons after emergence from the aperature possess little scattering with respect to velocity.

2. The edge of the beam originates at the edge of the aperture; the inner parts of the beam originate from the emission of the sections of the surface of the upper base of the cavity more distant from the aperture; the central parts originate from the lateral surfaces (see Fig. 6).

3. When anode voltages exceed 260 volts, emission from the edge of the aperture is saturated.

4. Within the range of voltages studied ($50 \leq V_A \leq 1000$ v) the current from the regions of the upper base of the cathode cavity located at a distance from the aperture greater than the radius of the aperture, and the current from the lateral surface, are bounded by a space charge.

5. The saturation of current from the regions indicated does not proceed at the same time. The boundary of the region of saturation migrates.

6. Variation of the geometric parameters of the cavity, namely its shape and the relationship of the dimensions, may produce a certain change in the structure of the beam.

We express our thanks to G. V. Spivak for his interest in the work and for a number of valuable suggestions and to Huang Kao-nien for his practical help in conducting the experiment.

Physics Dept; Lomonosov Moscow
State University

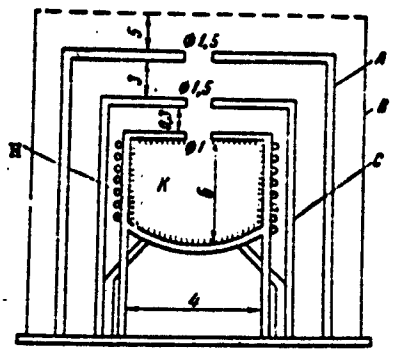

Fig. 1. Test gun with hollow cathode: A) anode; B) accelerating electrode; C) cold cathode; K) cathode; H) heater.

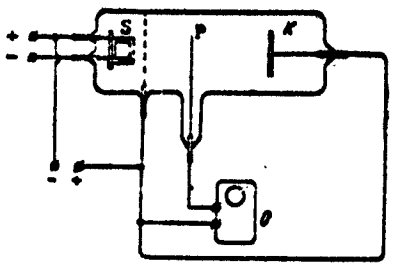

Fig. 2. Experimental tube and electrical circuit; S) electron gun with hollow cathode; P) probe; K) electron collector; O) oscilloscope.

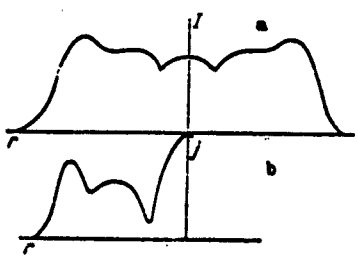

Fig. 3. Typical oscillogram of probe current (a); distribution of current density over the radius of the beam (b).

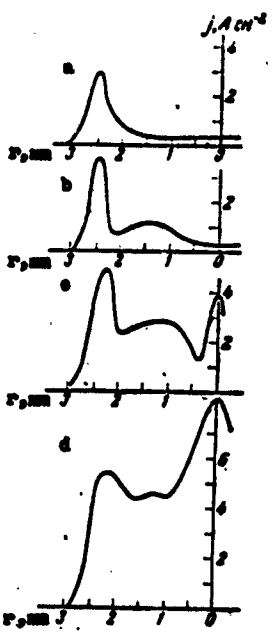

Fig. 4. Distribution of current density over the radius of the beam vs. anode voltage: a) V_A = 75v; b) V_A = 300v; c) V_A = 500v; d) V_A = 1000v.

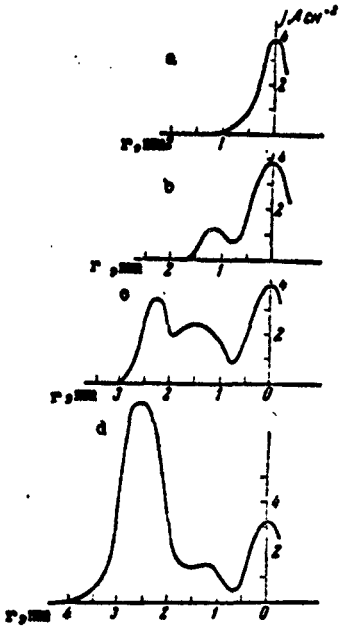

Fig. 5. Distribution of current density along the beam radius vs. the degree of heating of the cathode. Filament power: a) 6.4 watts; b) 11.9 w; c) 13.6 w; d) 20.4 w.

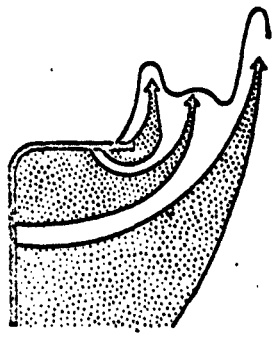

Fig. 6. Formation of electron flux from a hollow cathode.

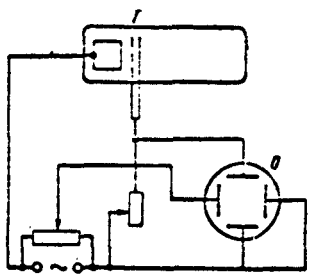

Fig. 7. Electrical circuit for recording volt-ampere characteristics of a hollow cathode: T) test diode; O) vertical plates of oscilloscope.

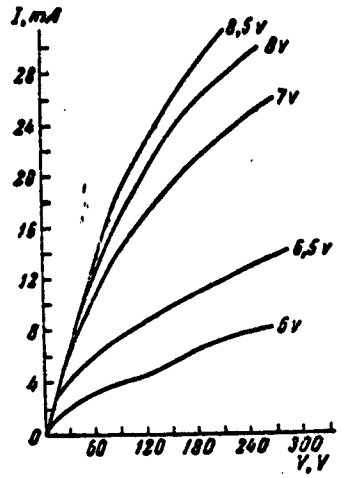

Fig. 8. Volt-ampere characteristics for different heating of the cathode (parameter — heater voltage).

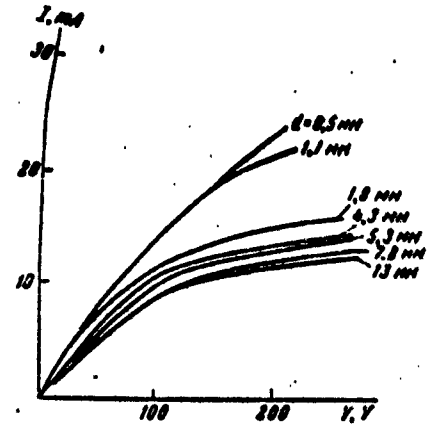

Fig. 9. Volt-ampere characteristics for various distances between the cathode and anode.

REFERENCES

1. A. Sandors. Proc. Inst. Electr. Engrs, B 108, 37, 90 (1961).

2. M. B. Pyt'yeva and Ye. M. Dubinina. Radiotekhnika i elektronika, No. 8, 1261, 1960.

3. J. Pierce. Voprosy radiolokatsionnoy tekhniki, No. 4, 52, 1955.

4. K. M. Poole. J. Appl. Phys., 26, No. 9, 1176 (1955).

5. I. K. Ovchinnokov. Ukr. fiz. zh., 4, No. 2, 226, 1959.

DISTRIBUTION LIST

DEPARTMENT OF DEFENSE	Nr. Copies
HEADQUARTERS USAF	
AFCIN-3D2	1
ARL (ARB)	1
OTHER AGENCIES	
CIA	1
NSA	6
DIA	9
AID	2
OTS	2
AEC	2
PWS	1
NASA	1
ARMY (FSTC)	3
NAVY	3
NAFEC	1
AFCRL (CRXLR)	1
PGE	12
RAND	1

MAJOR AIR COMMANDS	Nr. Copies
AFSC	
SCFDD	1
DDC	25
TDBTL	5
TDBDP	5
AEDC (AEY)	1
AFMTC (MTW)	1
AFWL (WLF)	1
APGC (PGF)	1
ASD (ASYIM)	2
ESD (ESY)	1
RADC (RAY)	1
SSD (SSF)	2
TDEPA (Smith)	1